Shahrood University of Technology

Journal of Mining and Environment (JME)

Journal homepage: www.jme.shahroodut.ac.ir

Iranian Society of Mining Engineering (IRSME)

Response of Underground Tunnels to Combined Dynamic Loadings of Running Metro-train and Earthquake

Rahul Shakya[1*], Manendra Singh[1] and Narendra Kumar Samadhiya[2]

1. Department of Civil Engineering, National Institute of Technology Hamirpur, Himachal Pradesh, India
2. Department of Civil Engineering, Indian Institute of Technology Roorkee, Uttarakhand, India

Article Info

Received 26 December 2022
Received in Revised form 2 January 2023
Accepted 10 January 2023
Published online 10 January 2023

DOI: 10.22044/jme.2023.12549.2277

Keywords

Dynamic loading
Underground tunnel
Metro-train
Time history
Earthquake

Abstract

An earthquake is a random occurrence that can happen anytime in highly seismic active areas. Therefore, it might happen even when the metro-train is moving. In such a scenario, the vibrations produced by the dynamic loading of a moving metro-train and the dynamic loading due to an earthquake will impact the dynamic response of underground metro-tunnels. In this work, an effort is made to comprehend how the Delhi Metro's underground tunnels will respond to the combined dynamic loading from the earthquake and the running train. Therefore, the dynamic response of underground metro-tunnels is primarily influenced by the vibrations generated due to the dynamic loading of a running metro-train and the dynamic loading due to an earthquake. Both these loadings cause vibrations at the ground surface and the tunnel utilities. In this paper, an attempt is made to understand the response of Delhi metro-underground tunnels to the combined dynamic loading due to the earthquake and the train's motion. Two-dimensional and three-dimensional finite element analyses are carried out using the Plaxis software. The research work finds that the overall response at the ground surface increases due to the combined dynamic loading of the train and earthquake compared to the train's or the earthquake's sole dynamic loading. Maximum displacements in the soil-the tunnel system and forces in RC liners are found to be more significant for the combined loading of the earthquake and the train motion than those due to individual loadings.

1. Introduction

Underground structures are important strategic components of utility and transportation networks. A new interest in researching how vulnerable these subsurface facilities are to seismic stress is brought on by the increased necessity in the recent years to expand these transit networks. The vulnerability of these structures to earthquakes is a highly delicate subject because of their importance. A significant earthquake could result in the loss of human life and damage to other infrastructure. This may lead to substantial financial losses, especially given how long it would take to get the network back up and running. An earthquake is a random occurrence, and can happen anytime in highly seismic active areas. Therefore, it might happen even when the metro-train is moving. In such a scenario, the vibrations produced by the dynamic loading of a moving metro-train and the dynamic loading due to an earthquake will impact the dynamic response of underground metro tunnels. In this work, an effort is made to comprehend how the Delhi Metro's underground tunnels will respond to the combined dynamic loading from the earthquake and the train's velocity. The speed of the moving train, the axle load of the wagons, and the wagon's length all impact the dynamic loading of a moving metro-train. These loads generate vibrations in the tunnel utilities and at the ground surface. Many researchers have investigated the influence of sole dynamic loading separately due to moving train and the influence of sole earthquake loading. Still, minimal studies have been conducted to find the effect of the combined dynamic loadings of an earthquake and a running metro-train. Therefore it

Corresponding author: rahulshakya4050@gmail.com (R. Shakya)

is very important to study the effect of combined dynamic loading on underground tunnels. In this paper, the effect of combined dynamic loadings of earthquake and running metro-train on Delhi metro-underground tunnels have been found by finite element method using finite element-based Plaxis software.

2. Review of Earlier Works

Metro-underground tunnels should be designed so that vibrations due to moving trains as well as due to earthquake do not cause any significant effect on the passengers traveling, the RC tunnel liners, other important equipment in the tunnels, the ground surface, and on the above-ground structures. It is, therefore, essential to reduce the effect of vibrations on the underground tunnel and the ground surface. Many researchers have investigated the influence of sole dynamic loading separately due to moving train and the influence of sole earthquake loading. However, it is always possible that an earthquake occurs simultaneously when the metro-train is in motion inside the tunnel. In this situation, the metro-tunnel is subjected to combined dynamic loadings of the moving train and the earthquake. Therefore, it is essential to investigate the effect of combined dynamic loadings on the dynamic response of metro-underground tunnels. The time history of the earthquake and running metro-train have not been combined into one-time history. Both time history loadings have been applied separately such that earthquake time history was applied at the base of the model and time history of running metro-train was applied at the bottom of the tunnel but at the same time. Several researchers have studied the train induced vibrations at the ground surface [1-18]. Some researchers developed analytical and finite element methods for the analysis with and without elastic foundations [19-23]. The district element method (DEM) has been widely used to investigate the mechanical behavior of geomaterials [24-26], and meshless methods were also used for the analysis [27-32]. Modelling and simulation can be the proficient alternative technique that provides solutions and insight into the various issues [33-34].

3. Dynamic Loadings of Metro-underground Tunnels

Underground metro-tunnels may be subjected to two types of dynamic loadings such as i) dynamic loading due to moving metro-train and ii) dynamic loading due to an earthquake.

3.1. Dynamic loading due to moving Delhi metro-trains

A longitudinal model of a moving train has been constructed by Nejati *et al*. [35]. In this model, the change in the normal force exerted by the wagon over time was computed, and the results were used to determine a point load that was applied to the base of the tunnel. The track-structure response induces a stress wave. Because of this, the vibrations that occurred at the contact between the wheel and the rail were utilized as a train of dynamic load, and other potential sources of vibrations were disregarded. This is because the effect of other vibration sources on dynamic wave loading is confined to the immediate area and is negligible. In other words, the most important parameters influencing the train's dynamic load features are the axle's weight, the distance between the wheel axles, and the train's speed.

In this paper, the Delhi metro-train has been considered for analysis. The schematic section of Delhi metro-train wagons is shown in Figure 1, along with the direction of the moving train. The reference point (origin) is assumed to be at $t = 0$ s. The properties of Delhi metro-train wagons are presented in Table 1. Each wagon wheel's axle force (F1) is assumed to be equal. As the train moves from right to left (as shown in Figure 1), the first wheel pair of the first train wagon applies a normal force of F_1 on the rail for a time interval (0, t_1). After a time, t_1, the normal force of the first pair of wagon wheels disappears until time, t_2, so that the normal axle force in the interval (t_1, t_2) is zero, and t_2 is the beginning of time when the second pair of wheels of the first wagon apply the normal force.

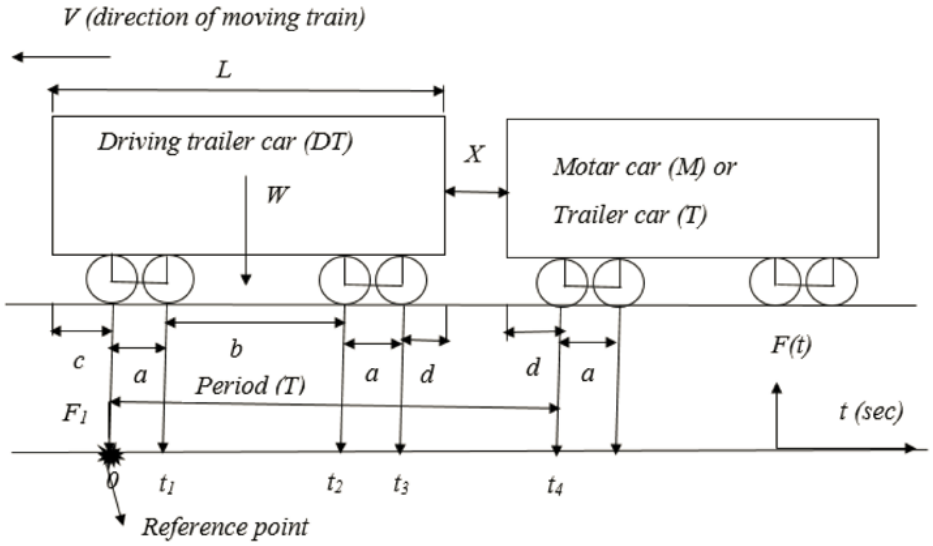

Figure 1. Planar view of Delhi metro-train wagons.

Table 1. Properties of Delhi metro-train.

Parameters	Symbol	Values
Metro-train formation		8 cars: DT-M-T-M-T-M-M-DT
Metro-train gauge		Broad gauge (1.676 m)
Dimensions		Length (L): 21.64m,
		Width: 3.2 m, Height: 3.898 m
Wheelbase	A	2.4 (m)
Bogie distance		15.0 (m)
	B	12.6 (m)
	C	2.12 (m)
	D	2.12 (m)
Distance between two cars	X	Approx. 0.5 m
Weight of wagon (tare)		Approx. 42 tons
Wight of the wagon with passengers	W	Approx. 70 tons
Axle load	F_1	$F_1 = W/8$ = 8.75 t = 87.5 kN
Performance		Max. Speed (V_{max}): 95 km/hr
		Acceleration: 0.8 m/s2
		(from 0 km/hr to 30 km/hr)
		Deacceleration:
		1.0 m/s^2 (service brake)
		1.3 m/s^2 (emergency brake)

Then, the normal axle force in the interval [t_2, t_3] is F_1. From time t_3 to t_4, the normal force of wagon wheels disappears. T_4 is the time of one complete cycle of the train forces. Therefore, the normal force of other train wagons can also be calculated similarly [35].

The function of the dynamic force of a metro train with time in the interval [0, t_4] is presented as [35]:

$$F(t) = \begin{cases} F_1 \ldots . 0 \le t \le t_1 \\ 0 \ldots . t_1 \le t \le t_2 \\ F_1 \ldots . t_2 \le t \le t_3 \\ 0 \ldots . t_3 \le t \le t_4 \end{cases} \quad (1)$$

$F(t)$ is a periodic function with a period equal to t_4. This function can be expressed as a Fourier series function, as given by Eq. 2 [36].

$$F(t) = a_0 + \sum_{n=1}^{\infty}\left[a_n \sin\left(\frac{2n\pi t}{T}\right) + b_n \cos\left(\frac{2n\pi t}{T}\right)\right] \quad (2)$$

where a_0, a_n, and b_n are the Fourier coefficients. These coefficients can be obtained from Eqs. 3a, 3b, 3c, which are:

$$a_0 = \frac{1}{T}\int_0^{t_4} F(t)dt \quad (3a)$$

$$a_n = \frac{2}{T}\int_0^{t_4} F(t)\cos(\omega_n)dt \quad (3b)$$

$$b_n = \frac{2}{T}\int_0^{t_4} F(t)\sin(\omega_n)dt \quad (3c)$$

where n is a natural number, and ω_n is the angular frequency of the dynamic train load.

$$\omega_n = \frac{2n\pi}{T} \quad (4)$$

Dynamic loading due to moving metro-trains was generated using Eq. (2), and thus presented in Figure 2. The maximum axle load was found to be 95.80 kN. The dynamic load of a metro-train is primarily influenced by the train's speed, axle load, and the length of the car.

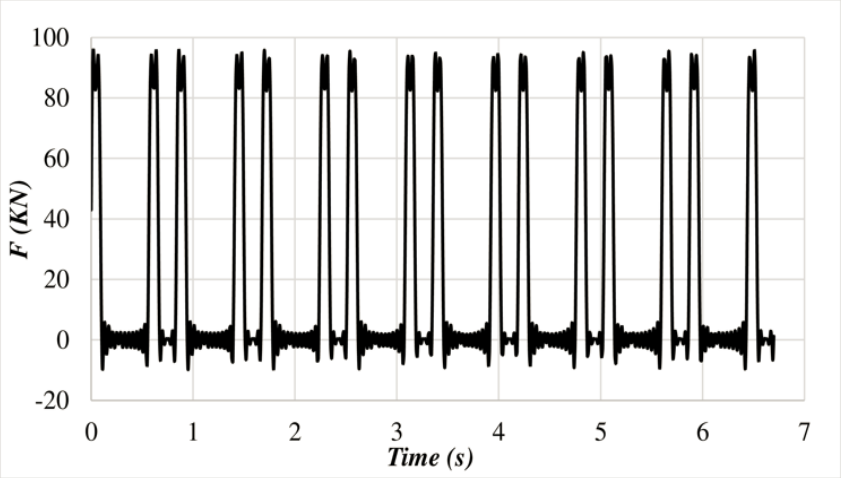

Figure 2. Dynamic loading of Delhi metro-train (Car weight = 70 t, speed = 95 km/hr, length of car = 21.64 m).

3.2. Dynamic loading due to earthquake

The most recent large earthquake was in 1999, which occurred at Chamoli, around 280 km from Delhi. Several Delhi structures had non-structural damage during this earthquake. The impacts of the Chamoli earthquake on Delhi show that Delhi is in danger of suffering significant damage from a sizable earthquake in the Himalayas. Therefore, it can be seen that Delhi is vulnerable to significant earthquake damage from both local earthquakes and major earthquakes that occur in the Himalayas. Thus the Chamoli earthquake in 1999, which had a magnitude of 6.8, was considered for the analysis. Figure 3a shows the acceleration-time history of the horizontal component of the 1999 Chamoli earthquake, which has a peak ground acceleration (PGA) of 3.53 m/s^2. This time-history graph was generated after applying the baseline correction. Acceleration-time history of the earthquake for which the analysis is being carried out should coincide with the acceleration-time history of the earthquake that is anticipated to occur at that site. An earthquake hit the Chamoli area of the Garhwal Himalaya in 1999. As per IS: 1893, Part 1 [37], the Chamoli district of the Garhwal Himalaya is located in zone V of the earthquake zoning map of India, and this map places Delhi in zone IV. Therefore, for zone IV, there is a need to create an entirely new artificial acceleration-time history.

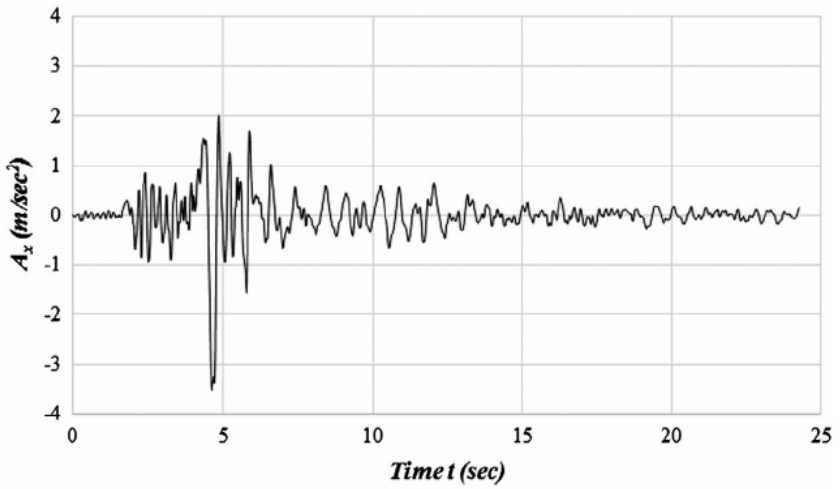

Figure 3a. Horizontal acceleration (A_x), Chamoli earthquake 1999.

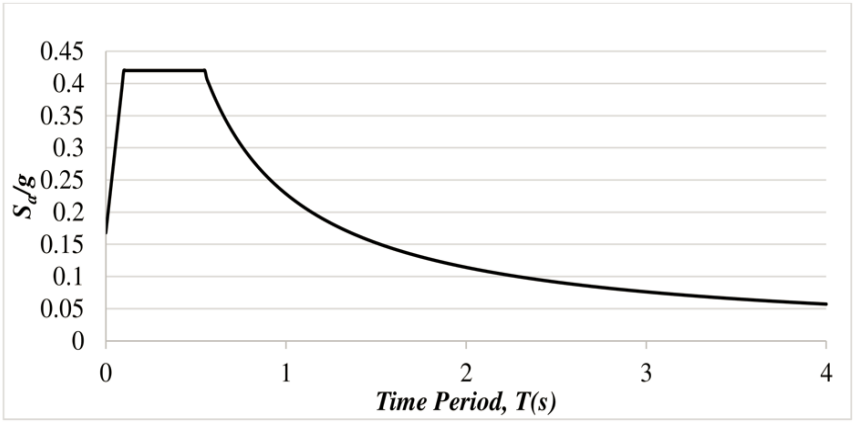

Figure 3b. Response spectra for zone IV for different damping ratios and for maximum considered earthquake [37].

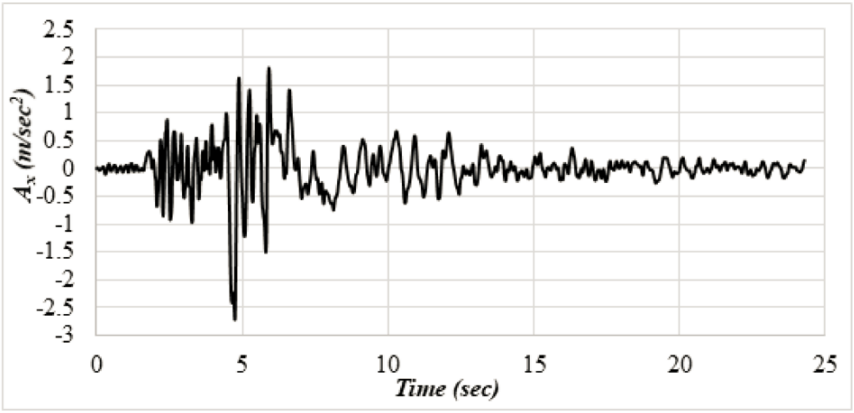

Figure 4. Artificial time history for horizontal component of Chamoli earthquake (1999).

Singh *et al*. [38] discussed generating response spectra compatible time history. Target response spectra of Delhi city were gathered as the initial phase in this process. The spectra of the target's response were created following IS: 1893, Part-1 [37] for the maximum considered earthquake (MCE). This spectrum was constructed based on the assumption that the damping ratio of Delhi silt is 15%. Taking the magnitude of acceleration from Figure 3b and phase from the given input time

history (Figure 3a), response spectra compatible time history was generated using the Siesmo Match software, and is presented in Figure 4. The updated time history preserves the earthquake's phase and time interval while decreasing the peak ground acceleration to 2.71 m/s^2.

4. 2-D Analysis of Delhi Metro-tunnels under Individual and Combined Dynamic Loadings

The tunnels beneath Connaught Place, New Delhi, between Rajiv Square and Patel Square, have been used as a representative site for this study of the Delhi Metro Rail Corporation (DMRC). Table 2 displays the tunnel segment's geometric characteristics. Parametric studies were conducted by adjusting the height of the overburden above the tunnel. As part of the preparation for the DMRC tunnels, large quantities of alluvium, often known as Delhi silt, were excavated. Table 3 summarizes the geotechnical properties of the medium soil that surrounds the tunnel.

In contrast to the soil's elastic modulus, which varied dramatically with depth, these characteristics are relatively constant. The elastic modulus changes as one travel further into the ground, as shown in Table 4. The tunnel was dug without hitting any water table. In Figure 5, we see the whole geometry of the physical model of the soil-tunnel system, along with representative sites at which different behavioral characteristics are monitored.

Table 2. Geometrical details of Delhi metro-tunnel [39, 40].

Properties	Magnitude
Width of tunnel, D	8.90 m
Height of Tunnel	6.44 m
Overburden depth, H	2 m, 10 m, 16 m
Support system	RC liners
RC liner's thickness	0.28 m
Elastic modulus of RC liners, E_c	3.16 x 10^7 kPa
RC liner's Poisson's ratio	0.15
Damping ratio	2.0 %

Table 3. Properties of soil medium surrounding Delhi metro-tunnel [39, 40].

Properties	Magnitude
Unit weight, γ_{bulk}	18 kN/m^3
Saturated unit weight, γ_{sat}	20 kN/m^3
Cohesion, c	0
Friction angle, φ	35°
Dilatational angle, ψ	5°
Poisson's ratio	0.25
Damping ratio	15.0%

Table 4. Elastic modulus's variation for Delhi silt with depth [39, 40].

Depth of stratum (m)	Thickness of stratum (m)	Elastic Modulus, E (MPa)
0-10	10	7.5
10-20	10	15.0
20-35	15	30.0
35-50	15	40.0
50-60	10	50.0

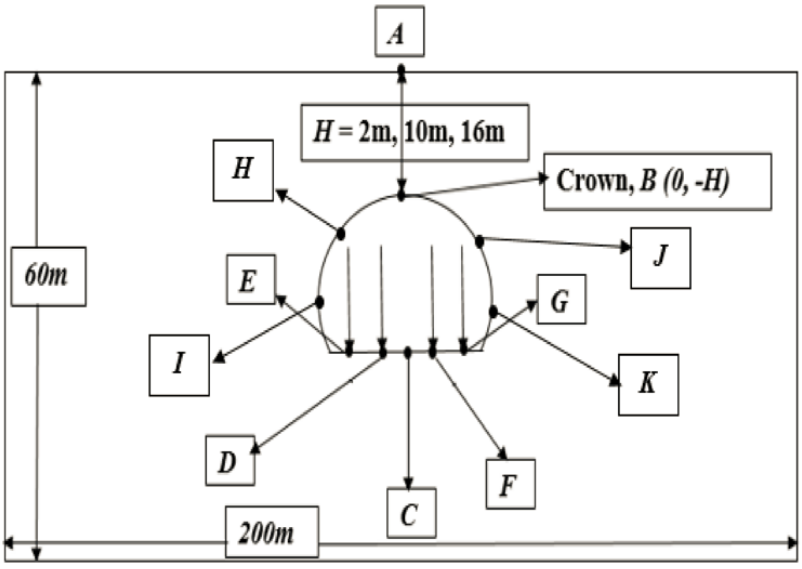

Figure 5. Geometry of physical model of the soil-the tunnel system with locations of monitoring points.

4.1. Numerical modelling

Using the Plaxis 2D software, a two-dimensional plane strain finite element analysis has been carried out to investigate the underground tunnels' response to the combined dynamic loading caused by the operation of the metro-trains and the earthquake. After conducting sensitivity analysis, the horizontal extent of the model was determined to be 200 m x 60 m. When modelling the soil domain, triangular elements with six nodes and an average size of 1.60 meters were considered. Kuhlemeyer & Lysmer [41] suggest that for optimal performance, a mesh's average element size should be smaller than or equal to one-eighth of the wavelength of the highest-frequency component of the input wave. (i.e. average element size $\leq \lambda/8$). In the present analysis, this criterion has been satisfied, and also the Authors have done the sensitivity analysis with different element sizes and reduced the element size to reach a stable result (i.e. 1.6 m), in which further reduction in element size gives the same result. The use of plate-bending elements [42] allowed for the simulation of segmental RC liners. In this study, the stress-strain behavior of soil was modeled as an elastoplastic system, which means that the Mohr-Coulomb yield criterion was applied. The elastic behavior of RC liners was taken into consideration. The assumption was made that there would be no slippage (a perfect bond) between the tunnel and the earth medium surrounding it. The damping in the tunnel's soil was calculated to be 15%, and the damping in the RC liners was assumed to be 2%.

4.1.1. Modeling of train dynamic loading

Two metro-trains are considered parallel to each other in the same direction on the underground tunnel. Dynamic loading of both moving trains was simulated by point loads, as shown in Figure 5. Dynamic loading of moving trains, as shown in Figure 5, was applied at the base of the tunnel at points D, E, F, and G.

4.1.2. Modeling of earthquake loading

Response spectra compatible time history presented in Figure 4 was applied at the model's base through prescribed displacements.

4.1.3. Boundary conditions

When considering the finite element mesh's static response, the nodes along the vertical borders were constrained in the horizontal (X) direction but allowed to move freely in the vertical (Y) direction. At the same time, the bottom boundary was fixed in both directions. For dynamic analysis, the displacement condition along both vertical boundaries was represented by the viscous absorbent boundary developed by Lysmer and Kulhemeyer [43]. The C1 and C2 absorbent border coefficients have been set to 1 and 0.25, respectively.

4.1.4. Steps of calculations

Analysis of underground metro tunnels to individual and combined loadings was carried out along the following lines:

Step 1: Only the initial in-situ state of stress was generated in this step. The tunnel and other loadings were kept inactive.

Step 2: The tunnel was excavated in this step, whereas dynamic loading was kept inactive.

Step 3: Dynamic loadings were applied to the soil-the-tunnel system. Three dynamic loading cases have been considered in this paper:

Case 1: Only the dynamic loading of moving trains was considered in this step. Dynamic loading of the metro train (Figure 2) was applied at the base of the tunnel.

Case 2: Only earthquake loading with the earthquake's horizontal (T) component (Figure 4) was applied at the model's base.

Case 3: Combined dynamic loadings due to the moving train and the horizontal component of the earthquake were considered. Both loadings were applied simultaneously. Dynamic loading of the metro-train (Figure 2) was applied at the base of the tunnel, while the horizontal component of the earthquake (Figure 4) was applied at the base of the model.

5. Results and Discussion

Results of the dynamic analysis of the underground metro-tunnel are presented in this section for three different cases of loading, as discussed in Section 4.1.4. The dynamic analysis results are discussed in the form of vertical displacement, vertical acceleration, vertical velocity, and forces in RC liners. Some specific points are selected at critical locations (Figure 5) such as at the ground surface (*A*), at the crown (*B*), at the bottom of the tunnel (*C*), and under the wheels of the first train (*D, E*), under the wheels of the second train (*F, G*), and around the periphery (*H, I, J, K*).

5.1. Response at ground surface

Response of the soil-the tunnel system was monitored at the ground surface regarding dynamic vertical displacement, vertical acceleration, and vertical velocity. Figure 6 shows the time history of dynamic vertical displacement at the ground surface (point *A*) for the depth of overburden, H = 16 m. The figure shows the time history of vertical displacement (U_z) for loading Cases 1, 2, and 3. Maximum values of dynamic vertical displacement at this point, *A,* is of the order of 3.162 mm in sole loading due to the train's motion at a speed of 95 km/hr and 4.744 mm in case of sole earthquake loading. When both loads act simultaneously, maximum vertical displacement has been found to increase to 6.978 mm. At the end of the earthquake and after the train's passage, there is a residual vertical displacement of about 2.2 mm. That result corresponds to vertical displacement only. Since the Horizontal component was applied at the base of the model, the earthquake's effect on vertical displacement at the ground surface was less.

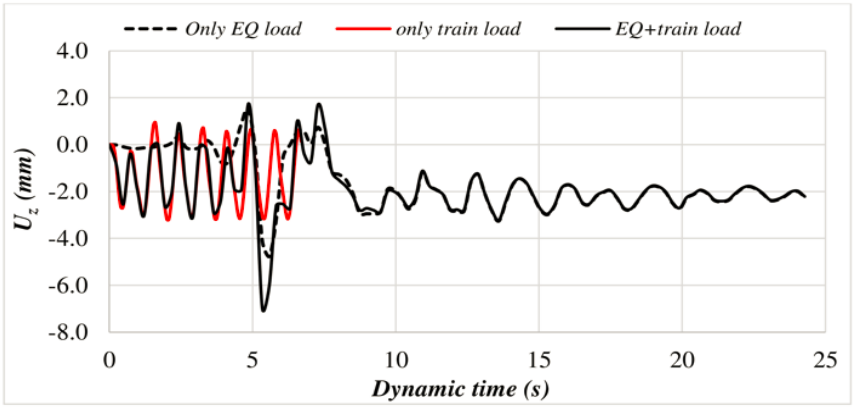

Figure 6. Vertical displacement at the ground surface (Case 1: only train load, Case 2: only EQ load, and Case 3: EQ + train load).

Similarly, the time history of vertical acceleration (A_z) at the ground surface has been presented in Figure 7. The values of vertical acceleration are 0.18 m/s^2, 0.063 m/s^2, and 0.192 m/s^2 corresponding to the three cases of only train dynamic loading, only earthquake loading, and the combined dynamic loadings. At the end of the earthquake and after the passage of the train, vertical acceleration reduces to zero.

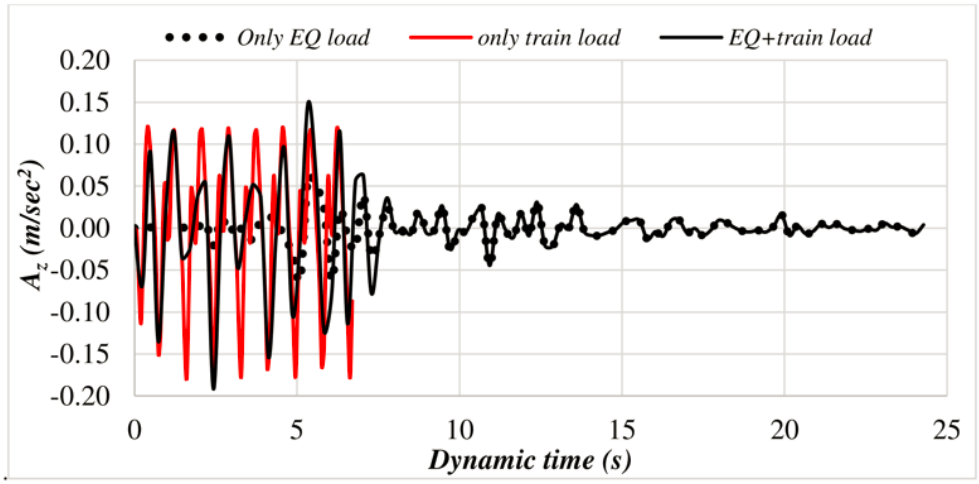

Figure 7. Vertical acceleration at the ground surface (Case 1: only train load, Case 2: only EQ load, and Case 3: EQ + train load).

Similarly, Figure 8 depicts the profile of variation of vertical velocity (V_z) with time at the ground surface. The respective values of velocity at the ground surface for the three cases of loading are 0.015 m/s, 0.017 m/s, and 0.03 m/s, respectively.

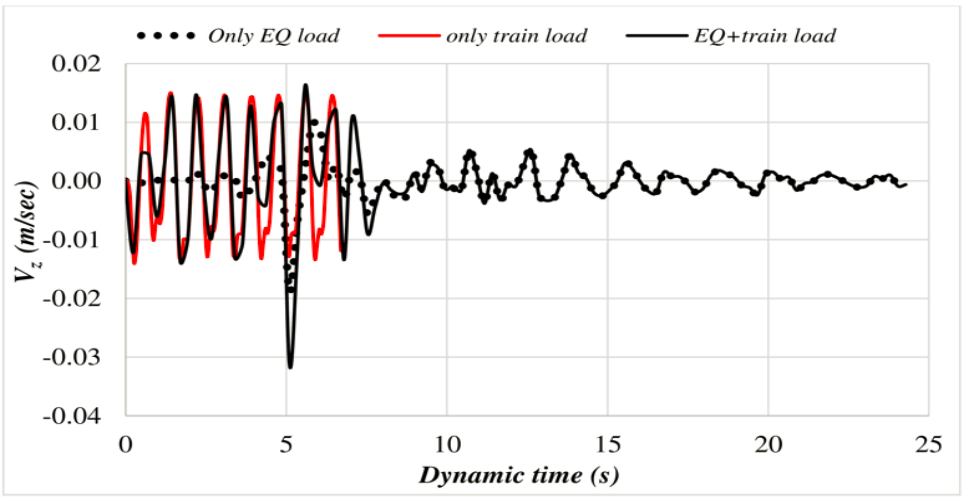

Figure 8. Vertical velocity at the ground surface (Case 1: only train load, Case 2: only EQ load, and Case 3: EQ + train load).

The response of the soil-tunnel system obtained at the ground surface has been compared for different values of depth of overburden above the tunnel. This comparison is presented in Table 5, from which it can be concluded that dynamic response generally reduces with an increase in overburden depth for all three cases of dynamic loading. Therefore, the depth of overburden is a critical issue for minimizing the effect of combined dynamic load at the ground surface. The depth of overburden should be so decided that the ground surface is not affected by the vibrations generated due to dynamic loadings.

Table 5. Response at the ground surface (Case 1: only train load, Case 2: only EQ load, and Case 3: EQ + train load).

H (m)	U_z (mm)			A_z (m/s^2)			V_z (m/s)		
	Case 1	Case 2	Case 3	Case 1	Case 2	Case 3	Case 1	Case 2	Case 3
2	8.327	4.210	11.000	0.998	0.770	1.178	0.060	0.019	0.065
10	4.622	4.152	8.302	0.276	0.069	0.227	0.021	0.018	0.030
16	3.163	4.744	6.978	0.179	0.063	0.192	0.015	0.017	0.029

5.1.2. Response around tunnel periphery

It can be found from the analysis that dynamic response was maximum at the invert of the tunnel (Point C). Therefore, the response has been compared for all cases of dynamic loadings. Time histories of dynamic vertical displacement, vertical acceleration, and vertical velocity at the tunnel invert are presented in Figures 9, 10, and 11, respectively, corresponding to the overburden depth, H = 16 m. It can be seen from these plots that the response at the tunnel invert is more significant for the case of sole dynamic loading of the train than that for sole earthquake loading or also for the combined loading due to train motion and earthquake. Especially the value of vertical acceleration for the sole dynamic loading of the train is significantly larger than that for Case 2 or Case 3. Response at the invert has also been compared for different values of overburden depth, and this comparison is presented in Table 6. It can be observed that vertical displacement, velocity, and acceleration are more significant for a lower overburden depth of 2 m, and after that, response values decrease with increasing overburden depth.

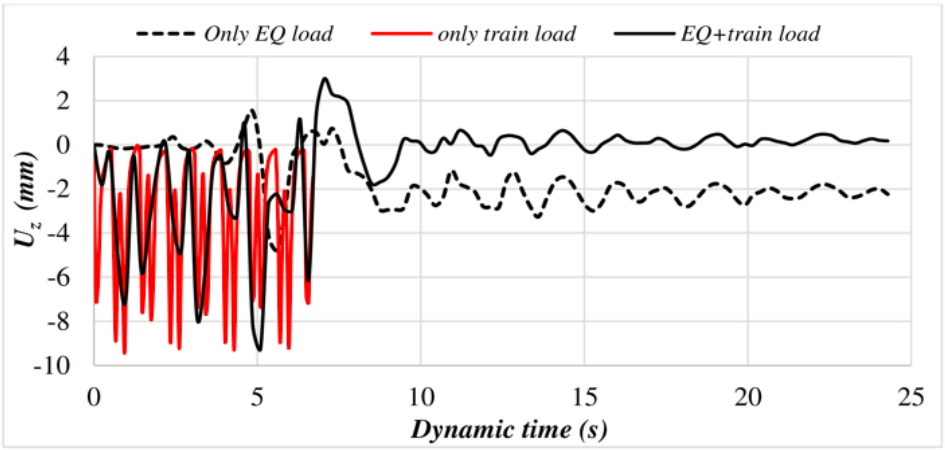

Figure 9. Vertical displacement at the tunnel invert (Case 1: only train load, Case 2: only EQ load, and Case 3: EQ + train load).

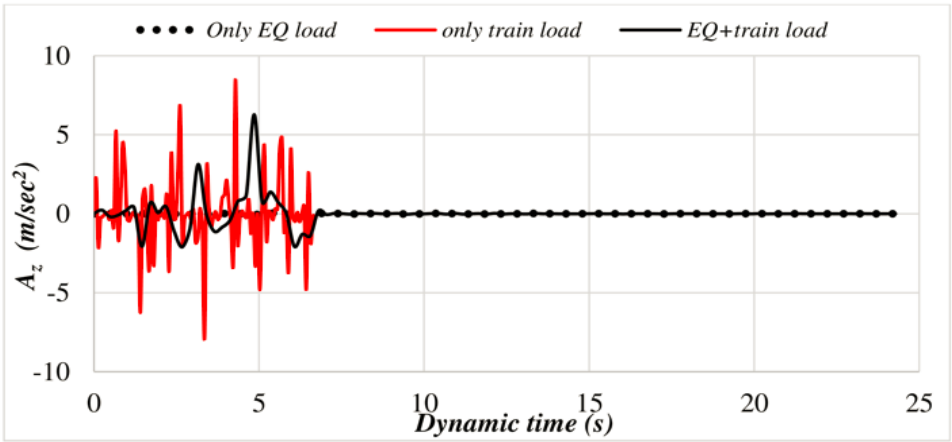

Figure 10. Vertical acceleration at the tunnel invert (Case 1: only train load, Case 2: only EQ load, and Case 3: EQ + train load).

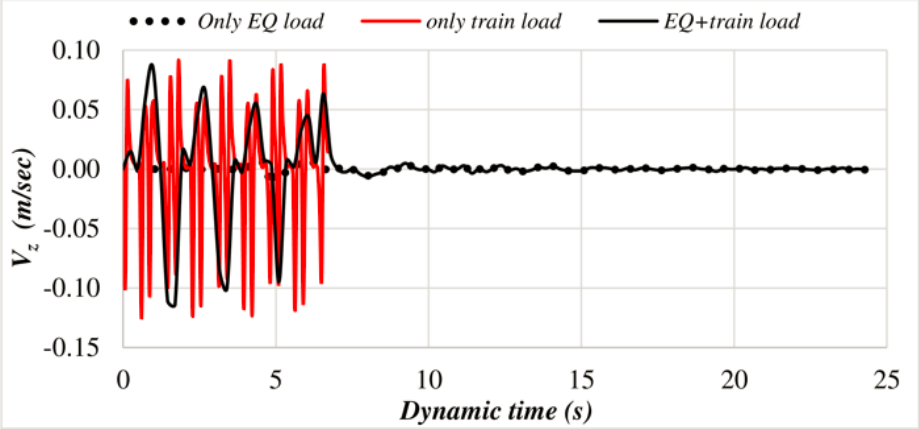

Figure 11. Vertical velocity at tunnel invert (Case 1: only train load, Case 2: only EQ load, and Case 3: EQ + train load).

Table 6. Response at the tunnel invert (Case 1: only train load, Case 2: only EQ load, and Case 3: EQ + train load).

H (m)	U_z (mm)			A_z (m/s^2)			V_z (m/s)		
	Case 1	Case 2	Case 3	Case 1	Case 2	Case 3	Case 1	Case 2	Case 3
2	17.00	2.78	15.00	16.70	0.078	10.23	0.208	0.015	0.208
10	12.00	2.70	12.00	13.69	0.076	9.83	0.176	0.014	0.167
16	9.24	1.96	9.25	8.51	0.067	6.28	0.126	0.012	0.114

5.1.3. Forces in RC liners

Dynamic forces mobilized in RC liners have also been presented in Table 7 for all three loading cases. Higher values of axial force (δT_{max}), shear force (δV_{max}), and bending moment (δM_{max}) have been obtained in RC liners for the case of combined loading. It can also be noticed that this increment in dynamic forces reduces with an increase in the overburden depth of the tunnel. Therefore, the combination of train and earthquake loadings is more critical for lesser overburden depth.

Table 7. Dynamic forces in RC liners (Case 1: only train load, Case 2: only EQ load, and Case 3: EQ + train load).

H (m)	δT_{max}(kN/m)			δV_{max} (kN/m)			δM_{max} (kN-m/m)		
	Case 1	Case 2	Case 3	Case 1	Case 2	Case 3	Case 1	Case 2	Case 3
2	19.92	44.34	62.06	11.92	95.89	98.82	18.15	42.74	49.99
10	6.53	43.71	46.24	6.53	89.98	91.07	8.08	39.87	45.52
16	10.00	2.00	12.00	6.11	85.87	86.25	6.77	11.04	14.47

Table 8 shows the generated axial force and a bending moment of the RC liner of the tunnel in static conditions as well as in all three cases of dynamic loadings. Combined axial and bending stress in RC liners have been calculated and shown in Table 8. The induced combined stresses have been compared with the permissible limit of M40 concrete [44], as shown in Figure 12. It can be observed in Table 8 and Figure 12 that the combined axial and bending stress in RC liners have been calculated to be 21.91 MPa, 22.20MPa and 22.50MPa for Case 1, Case 2 and Case 3, respectively. The forces and displacements in RC liners have increased significantly during the dynamic loadings. Still, stresses in the RC liners of the tunnel do not exceed their permissible limit in M40 concrete, and hence, the tunnel's liners are safe. However, combined axial and bending stresses in RC liners are very close to their permissible value in the case of combined dynamics loading.

Table 8. Combined stress in RC liner due to the axial force and bending moment (Case 1: only train load, Case 2: only EQ load, and Case 3: EQ + train load).

Force	T_{max} (kN/m)	M_{max}(kN-m/m)	Combined axial and bending stress in RC liner (MPa)
Static Value	1030	231	21.36
Case 1	1040	237.77	21.91
Case 2	1032	242.04	22.20
Case 3	1042	245.47	22.50

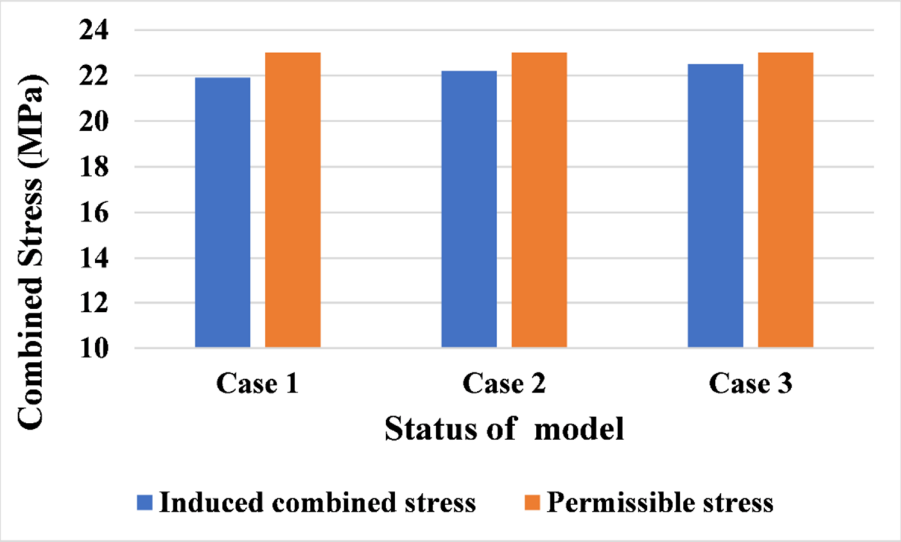

Figure 12. Variation of combined stress in RC liner.

5.2. Three-dimensional analysis of tunnels

For a more realistic response, the longitudinal direction of the tunnel is very important. Therefore, three-dimensional analysis of the metro-underground tunnel is necessary. The same problem in the two-dimensional study has been analyzed again. The tunnel length is three times the length of the metro-train, i.e. 518.4 m.

5.2.1. Numerical modelling

To perform a three-dimensional finite element analysis utilizing the Plaxis 3D software, the extent of the model has been determined to be 200 m x 518.4 m x 60 m in the X, Y, and Z directions, respectively. This was done after carrying out the sensitivity analysis. For the modelling of the soil domain, tetrahedral elements with 10 nodes were utilized. The stress-strain behavior of soil was thought to be elastoplastic, which means that the Mohr-Coulomb yield criterion was used to evaluate it. The RC liners were linearly elastic. The assumption was made that there would be no slippage between the soil medium around the tunnel and the tunnel itself. Nodes along the XZ plane of the model were constrained in the Y direction for the static response, but they were free to move in the X and Z directions.

On the other hand, nodes along the YZ plane of the model were constrained in the X direction for the static response but they were free to move in the Y and Z directions. The lower boundary was constrained in all directions, whereas the upper surface was allowed to remain unrestricted in all directions. The viscous absorbent border presented by Lysmer and Kuhlmeyer [43] was used for the dynamic response to represent the displacement condition along both vertical planes. This was done to keep the analysis as simple as possible (XZ and YZ planes). Two metro-trains that are said to be running parallel to each other in the tunnel have been considered for the analysis. As was stated in two-dimensional analyses, a simulation of dynamic loading was performed using line load on both moving trains. In this scenario, the length of the tunnel is, in contrast, equivalent to three times that of the metro- train. The following three scenarios of loading have been taken into consideration for the study:

Case A: The first portion of the tunnel is loaded by the dynamic load of the running metro-train, as shown in Figure 13a.

Case B: Middle portion of the tunnel is loaded by the dynamic load of the running metro-train (Figure 13b), and

Case C: The last portion of the tunnel is loaded by the dynamic load of the running metro-train, as shown in Figure 13c.

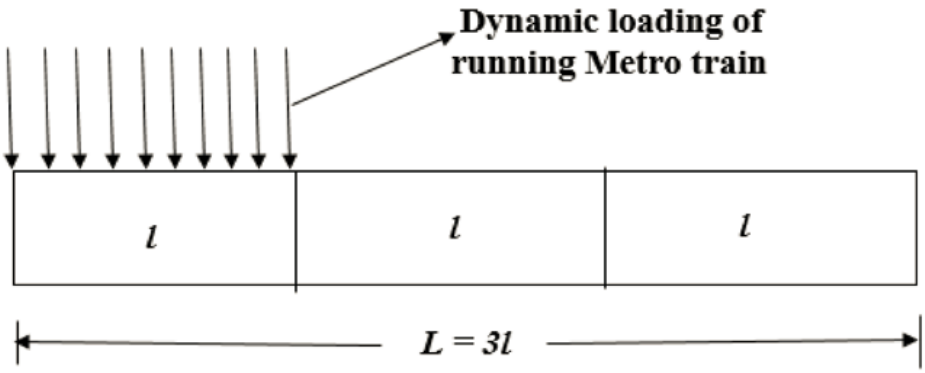

Figure 13a. Schematic diagram of loading condition on tunnel (Case A).

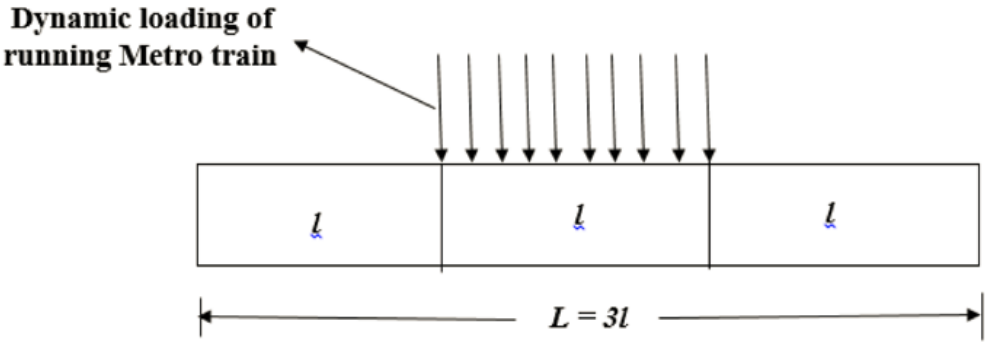

Figure 13b. Schematic diagram of loading condition on tunnel (Case B).

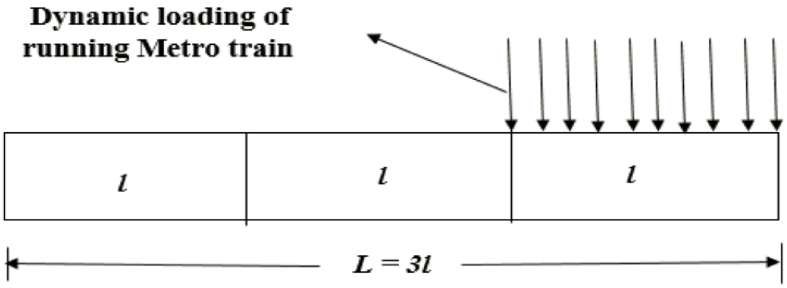

Figure 13c. Schematic diagram of loading condition on tunnel (Case C).

Figures 13a, b, and c only show the outline diagram in 1D. Not a single line load was considered. Two-line loads for each metro-train and four-line loads for two metro-trains were considered. These two-line loads correspond to the series of point loads of two train axles.

5.2.2. Displacements at end of dynamic loadings

Values of residual displacements in the soil-tunnel system for different dynamic loadings have been tabulated in Table 9. Horizontal and vertical displacements in the soil medium and RC liners are greater for combined loadings than for any individual loading. The effect of dynamic loadings on longitudinal displacement is negligible.

Table 9. Maximum dynamic residual displacements in soil-tunnel system at the end of dynamic loadings.

U (mm)		Only train loading (Case A)	EQ loading alone	Combined loading
Soil medium	U_x (mm)	1.45	255.80	270.60
	U_y (mm)	0.45	125.00	126.30
	U_z (mm)	2.82	4.00	4.71
RC liners	U_x (mm)	1.01	46.38	56.62
	U_y (mm)	0.19	0.36	0.36
	U_z (mm)	2.82	1.30	3.78

5.2.3. Displacements at ground surface during dynamic loadings

Maximum values of horizontal displacement, vertical displacement, longitudinal displacement (U_y), horizontal acceleration, and vertical acceleration have been obtained for all critical points (Figure 14a) at the ground surface. Maximum values of displacements and accelerations from these points have been selected and compared in Table 10 for different dynamic loadings. Values of longitudinal and vertical displacements are significantly greater for the combined loading than those due to individual loading, whereas horizontal displacement and horizontal acceleration are slightly higher for the combined loading than those for the individual loading. Vertical acceleration for combined loading is the same as that of the individual loading due to running a metro-train.

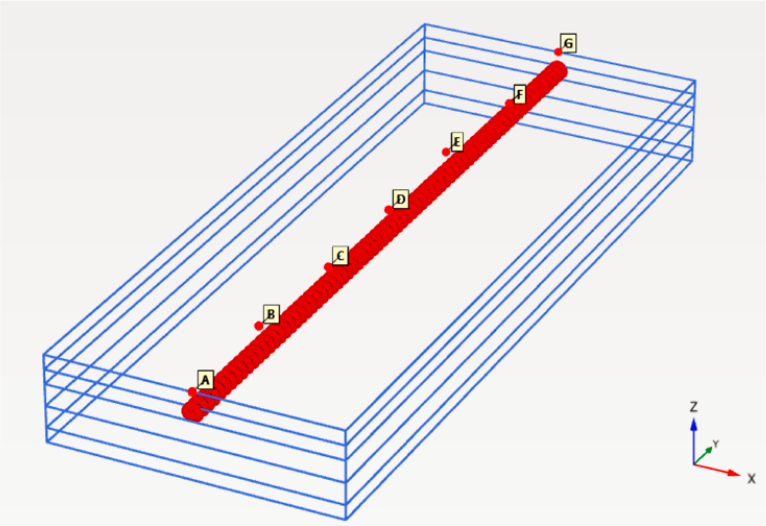

Figure 14a. Critical points at ground surface.

Table 10. Maximum dynamic displacements at ground surface during different dynamic loadings.

Response	Only train loading (Case A)	EQ loading alone	Combined loading
U_x (mm)	0.43	356	358
U_y (mm)	0.84	49	73
U_z (mm)	4.47	36	61
A_z (m/s^2)	0.35	0.19	0.35
A_x (m/s^2)	0.02	1.99	2.04

5.2.4. Displacements around tunnel periphery during dynamic loadings

The maximum response around the periphery of the tunnel during the dynamic loadings has been obtained at cross-section Y= 0 for all critical points (Figure 14b). It can be observed that the horizontal displacement, U_x is maximum at point 7, longitudinal displacement, U_y, and vertical displacement, U_z is maximum at point 3 (the tunnel invert), and values of horizontal and vertical acceleration are maximum at point 1 (the tunnel invert). Afterwards, the maximum dynamic response at these critical points (Points 7, 3, and 1) has been studied at different cross-sections along the length of the tunnel, i.e. Y = 0, 86.4, 172.8,

259.2, 345.6, 432.0, and 518.4 m. It can be found that the horizontal, U_x and vertical, U_z displacements and horizontal and vertical acceleration are maximum at the cross-section, Y=86.4 m along the length of the tunnel, i.e. at the mid-point of train length. Longitudinal displacement is maximum at cross-section Y= 0 along the tunnel's length, i.e. the tunnel's starting point.

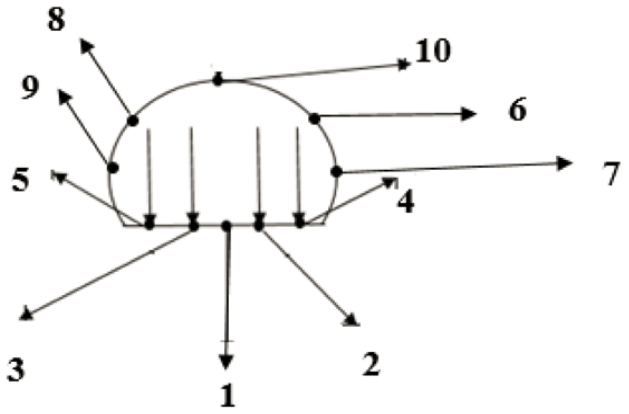

Figure 14b. Critical points around tunnel periphery at cross-section, Y = 0.

Therefore, maximum response around the periphery of the tunnel has been compared for the different types of dynamic loadings. Table 11 gives the maximum values of displacements and acceleration in RC liners of the tunnel. These are slightly higher for combined loading than for individual loading of running metro-trains or earthquakes, except for vertical acceleration.

Table 11. Maximum dynamic response of the tunnel during different dynamic loadings.

Response	Only train loading (Case A)	EQ loading alone	Combined loading
U_x (mm)	2.64	331	333
U_y (mm)	0.31	0.71	1.95
U_z (mm)	12	1.86	12.0
A_z (m/s^2)	12.04	0.037	12.2
A_x (m/s^2)	0.16	1.89	2.04

5.2.5. Dynamic forces in RC liners

Dynamic shear forces in RC liners of the tunnel have increased significantly due to combined loadings. These are higher for combined loading than for individual loadings (Table 12).

In Table 12, N_1 represents the axial force in the Y-direction, N_2 represents the force perpendicular to the tunnel axis, (Y), Q_{12} represents the in-plane shear force in the YZ plane, Q_{13} represents the shear force in the XY plane, Q_{23} represents the shear force in the YZ plane, M_{11} represents the bending moment due to bending about the Z-axis (around Z-axis), M_{22} represents the bending moment due to bending about X-axis and M_{12} represents the torsional moment according to transverse shear force.

Table 12. Maximum dynamic forces in RC liners of the tunnel for different dynamic loadings.

Forces	Only train loading (Case A)	EQ loading alone	Combined loading
N_1 (kN)	-1.9	17.6	11.4
N_2 (kN)	-0.71	-31.9	6.73
Q_{12} (kN)	-3.0	-27.4	-28
Q_{23} (kN)	130.3	0.6	144.2
Q_{13} (kN)	17	63	76
M_{11} (kN-m)	1.73	-0.01	1.78
M_{22} (kN-m)	-2.0	10.0	9.0
M_{12} (kN-m)	-0.1	2.6	2.5

6. Conclusions

Two-dimensional analyses of the Delhi metro-underground tunnels for different cases of dynamic loading have led to the following significant conclusions:

i) Response to sole dynamic loading of moving train (Case 1) in terms of dynamic vertical displacement, vertical acceleration, and vertical velocity is greater at the bottom of the tunnel (invert) than at the ground surface and the crown. The overall response at all the critical points decreases with the increase in overburden depth. Forces in RC liners have been found to increase due to the sole dynamic loading of the train, and these forces reduce with an increase in depth of overburden.

ii) The overall response at the ground surface was found to increase due to the combined dynamic loading of the train (Case 3) and the horizontal component of the earthquake as compared to that of the sole dynamic loading of the train (Case 1) and earthquake alone (Case 2). This response reduces with the increase in overburden depth for all three cases of dynamic loadings. Therefore, for minimizing the effect of dynamic loadings at the ground surface, the selection of overburden depth is very critical. The overburden depth of the tunnel should be so carefully chosen that the ground surface is not affected by the dynamic loading in an underground metro tunnel.

iii) Dynamic forces in RC liners obtained for the combined loading of the train and horizontal component of the earthquake (Case 3) were found to be higher than those of sole dynamic loading of the train (Case 1), and the only horizontal component of the earthquake (Case 2).

iv) The forces and displacements in RC liners have been increased significantly during the individual dynamic loadings but combined axial and bending stresses in RC liners do not exceed their permissible limit in M40 concrete. Hence, the tunnel's liners are safe. However, combined axial and bending stresses in RC liners are very close to their permissible value in the case of combined dynamics loading.

The response of 3-D analysis of metro-underground tunnels subjected to dynamic loadings has been summarized below:

i) Maximum residual displacements in soil-the tunnel system have increased significantly due to combined loadings of running metro-train and earthquake.

ii) Maximum displacements in the soil-the tunnel system and forces in RC liners were found to be greater for the combined loading of the earthquake and running metro-tunnel than those for the individual loadings.

Statements and Declarations
Funding:

The authors received no financial support for this article's research work, authorship, and publication.

Conflicts of interest:

The authors declare no conflict of interest.

Availability of data and material:

All the data used in this study are available from the corresponding author upon reasonable request.

Author's contribution:

All authors contributed equally to this work.

References

[1]. Kalantarian, S.H. and Dehghani, M. (2014). Review on the dynamic vibrations relationship in the metro tunneling. Int. J. of Science and Engineering Investigations. 3 (27): 23-27.

[2]. De-yun, D., Wei-ning, L., Gupta, S., Lombaert, G., and Degrande, G. (2010). Prediction of vibrations from underground trains on Beijing metro line 15. J. Cent. South Univ. Technology, 17, 1109−1118.

[3]. Nicolosia. V., D'Apuzzob, M., and Bogazzi, E. (2012). A Unified approach for the prediction of vibration induced by underground metro. Procedia - Social and Behavioral Sciences, 53, 62 – 71.

[4]. Nejati, H.R., Ahmadi, M., Hashemolhosseini, H., and Hayati, M. (2012a). Probabilistic analysis of ground surface vibration due to train movement, a case study on Tehran metro line 4. Geotech. Geology Engg. 30 (5): 1137–1146.

[5]. Wu, D., and Gao, B. (2013). Dynamic analysis of the tunnel entrance under the effect of Rayleigh wave. EJGE, 18, 4231-4246.

[6]. Metrikine, A.V. and Vrouwenvelder, A.C. W.M. (2000). Surface ground vibration due to a moving train in a tunnel: two-dimensional model. J. of Sound and vibration. 234 (1): 43–66.

[7]. Gardien, W. and Stuit, H. G. (2003). Modelling of soil vibrations from railway the tunnels. J. Sound and Vibration. 267 (3): 605–619.

[8]. Hall, L. (2003). Simulations and analyses of train-induced ground vibrations in finite element models. Soil Dynamics and Earthquake Engineering. 23 (5): 403–413.

[9]. Sheng, X., Jones, C.J.C., and Thompson, D.J. (2004). A theoretical study on the influence of the track on train-induced ground vibration. J. of Sound and Vibration. 272 (3-5): 909–936.

[10]. Sheng, X., Jones, C.J.C., and Thompson, D.J. (2006). Prediction of ground vibration from trains using the wavenumber finite and boundary element methods. J. of Sound and Vibration. 293 (3-5): 575–586.

[11]. Forrest, J.A. and Hunt, H.E.M. (2006). A three-dimensional the tunnel model for calculation of train-induced ground vibration. J. of Sound and Vibration. 294 (4-5): 678–705.

[12]. Forrest, J.A. and Hunt, H.E.M. (2006b). Ground vibration generated by trains in underground tunnels. J. of Sound and Vibration. 294 (4-5): 706–736.

[13]. Andersen, L., and Jones, C.J.C (2006). Coupled boundary and finite element analysis of vibration from railway the tunnels-a comparison of two- and three-dimensional models. J. of Sound and Vibration. 293 (3-5): 611–625.

[14]. Hussein, M.F.M. and Hunt, H.E.M. (2007). A numerical model for calculating vibration from a railway the tunnel embedded in a full-space. J. of Sound and Vibration. 305 (3): 401–431.

[15]. Ma, M., Markine, V., Liu, W., Yuan, Y., and Zhang, F. (2011). Metro train-induced vibrations on historic buildings in Chengdu. China. J. Zhejiang Univ. – Sci. A (Applied Phys & Eng). 12 (10): 782-793.

[16]. Wolf, S. (2003). Potential low frequency ground vibration (f = 63 Hz) impacts from underground LRT operations. J. of Sound and Vibration, 267, 651–661.

[17]. Taiyue, Q.I. and Gao, B. (2011). Strata consolidation subsidence induced by metro tunneling in saturated soft clay strata. J. of Modern Transportation. 19 (1): 35-41.

[18]. Mazek, S.A. and Almannaei, H.A. (2013). Finite element model of Cairo metro tunnel-Line 3 Performance. Ain Shams Engineering Journal, 4(4): 709–716.

[19]. Yaylacı, E.U., Yaylacı, M., Ölmez, H., and Birinci, A. (2020). Artificial neural network calculations for a receding contact problem. Computers and Concrete, An International Journal. 25 (6): 551-563.

[20]. Yaylaci, M., Yayli, M., Uzun Yaylaci, E. O lmez, H., and Birinci, A. (2021b). Analyzing the contact problem of a functionally graded layer resting on an elastic half plane with theory of elasticity, finite element method and multilayer perceptron. Struct. Eng. Mech. 78 (5): 585-597.

[21]. Birinci, A., Adıyaman, G., Yaylacı, M., and Öner, E. (2015). Analysis of continuous and discontinuous cases of a contact problem using analytical method and FEM. Latin American Journal of Solids and Structures, 12, 1771-1789.

[22]. Oner, E., Yaylaci, M., and Birinci, A. (2015). Analytical solution of a contact problem and comparison with the results from FEM. Structural engineering and mechanics: An international journal. 54 (4): 607-622.

[23]. Yaylacı, M., Eyüboğlu, A., Adıyaman, G., Yaylacı, E.U., Öner, E., and Birinci, A. (2021). Assessment of different solution methods for receding contact problems in functionally graded layered mediums. Mechanics of Materials, 154, 103730.

[24]. Öner, E., Yaylacı, M., and Birinci, A. (2014). Solution of a receding contact problem using an analytical method and a finite element method. Journal of Mechanics of Materials and Structures. 9 (3): 333-345.

[25]. Yaylaci, M., Adiyaman, G., Oner, E., and Birinci, A. (2020). Examination of analytical and finite element solutions regarding contact of a functionally graded layer. Structural Engineering and Mechanics. 76 (3): 325-336.

[26]. Yaylaci, M. (2022). Simulate of edge and an internal crack problem and estimation of stress intensity factor through finite element method. Advances in nano research. 12 (4): 405-414.

[27]. Adıyaman, G., Birinci, A., Öner, E., and Yaylacı, M. (2016). A receding contact problem between a functionally graded layer and two homogeneous quarter planes. Acta Mechanica. 227 (6): 1753-1766.

[28]. Yaylaci, M., Adiyaman, G., Oner, E., and Birinci, A. (2021). Investigation of continuous and discontinuous contact cases in the contact mechanics of graded materials using analytical method and FEM. Computers and Concrete. 27 (3): 199-210.

[29]. Yaylaci, M. and Birinci, A. (2013). The receding contact problem of two elastic layers supported by two elastic quarter planes. Structural engineering and mechanics: An international journal. 48 (2): 241-255.

[30]. Yaylacı, M. (2016). The investigation crack problem through numerical analysis. Structural Engineering and Mechanics, An Int'l Journal. 57 (6): 1143-1156.

[31]. Yaylaci, M., Abanoz, M., Yaylaci, E. U., Olmez, H., Sekban, D. M., and Birinci, A. (2022). The contact problem of the functionally graded layer resting on rigid foundation pressed via rigid punch. Steel and Composite Structures. 43 (5): 661–672

[32]. Öner, E., Şengül Şabano, B., Uzun Yaylacı, E., Adıyaman, G., Yaylacı, M., and Birinci, A. (2022). On the plane receding contact between two functionally graded layers using computational, finite element and artificial neural network methods. ZAMM-Journal of Applied Mathematics and Mechanics/Zeitschrift für Angewandte Mathematik und Mechanik. 102 (2): e202100287.

[33]. Yaylaci, M., Sabano, B.S., Ozdemir, M.E., and Birinci, A. (2022). Solving the contact problem of functionally graded layers resting on a HP and pressed with a uniformly distributed load by analytical and numerical methods. Structural Engineering and Mechanics. 82 (3): 401-416.

[34]. Yaylacı, M., Abanoz, M., Yaylacı, E.U., Ölmez, H., Sekban, D.M., and Birinci, A. (2022). Evaluation of the contact problem of functionally graded layer resting on rigid foundation pressed via rigid punch by analytical and numerical (FEM and MLP) methods. Archive of Applied Mechanics. 92 (6): 1953-1971.

[35]. Nejati, H.R., Ahmadi, M., and Hashemolhosseini, H. (2012b). Numerical analysis of ground surface vibration induced by underground train movement. Tunneling and Underground Space Technology, 29, 1-9.

[36]. Duffy, D.G. (2012). Advanced Engineering Mathematics. CRC Press.

[37]. IS: 1893 – 2002 (Part - 1). Criteria for Earthquake Resistant Design of Structures. Bureau of Indian Standards, Manak Bhawan, New Delhi.

[38]. Singh, M., Viladkar, M.N., and Samadhiya, N.K. (2017). Seismic response of metro underground tunnels. Int. J. of Geotech. Engg. 11 (2): 175-185.

[39]. Sony, S. (2015). Static and dynamic response of Delhi metro tunnels. Ph.D. thesis IIT Delhi.

[40]. Yadav, H.R. (2005). Geotechnical Evaluation of Delhi Metro tunnels. Ph.D. Thesis Department of Civil Engineering, IIT Delhi, India.

[41]. Kuhlemeyer, R. L. and amp; Lysmer, J. (1973). Finite element method accuracy for wave propagation problems. Journal of the Soil Mechanics and Foundations Division. 99 (5): 421-427.

[42]. Cen, S., and amp; Shang, Y. (2015). Developments of Mindlin-Reissner plate elements. Mathematica Problems in Engineering, 2015

[43]. Lysmer, J. and Kuhlemeyer, R.L. (1969). Finite dynamic model for infinite media. Journal of the engineering mechanics division. 95 (4): 859-877.

[44]. IS: 456 (2000). Plain and reinforced concrete-Code of Practice. Bureau of Indian Standards, New Delhi, India.

واکنش تونل‌های زیرزمینی به بارگذاری‌های دینامیکی ترکیبی قطار مترو در حال حرکت و زلزله

راهول شاکیا[1*]، ماناندرا سینگ[1] و نارندرا کومار سامدیا[2]

۱. گروه مهندسی عمران، موسسه ملی فناوری حمیرپور، هیماچال پرادش، هند

۲. گروه مهندسی عمران، موسسه فناوری هند رورکی، اوتاراکند، هند

ارسال۲۰۲۲/۱۲/۲۶، پذیرش۲۰۲۳/۰۱/۱۰

* نویسنده مسئول مکاتبات: rahulshakya4050@gmail.com

چکیده:

زمین لرزه یک رویداد تصادفی است که می‌تواند در هر زمان در مناطق با لرزه شدید فعال رخ دهد. بنابراین، حتی زمانی که قطار مترو در حال حرکت است، ممکن است این اتفاق بیفتد. در چنین سناریویی، ارتعاشات ناشی از بارگذاری دینامیکی یک متروی در حال حرکت و بارگذاری دینامیکی ناشی از زلزله بر پاسخ دینامیکی تونل‌های مترو زیرزمینی تأثیر می‌گذارد. در این کار، تلا شی برای درک چگونگی پا سخ تونل‌های زیرزمینی مترو دهلی به بارگذاری دینامیکی ترکیبی از زلزله و قطار در حال حرکت انجام شده است. بنابراین، پاسخ دینامیکی تونل‌های زیرزمینی مترو عمدتاً تحت تأثیر ارتعاشات ایجاد شده در اثر بارگذاری دینامیکی قطار مترو در حال حرکت و بارگذاری دینامیکی نا شی از زلزله است. هر دو این بارگذاری‌ها باعث ایجاد ارتعاش در سطح زمین و تا سیسات تونل می شوند. در این مقاله سعی شده است واکنش تونل‌های زیرزمینی مترو دهلی به بارگذاری دینامیکی ترکیبی نا شی از زلزله و حرکت قطار مورد مطالعه قرار گیرد. تجزیه و تحلیل المان محدود دو بعدی و سه بعدی با استفاده از نرم افزار Plaxis انجام شد. کار تحقیقاتی نشان می‌دهد که پاسخ کلی در سطح زمین به دلیل بارگذاری دینامیکی ترکیبی قطار و زلزله در مقایسه با بار دینامیکی قطار یا تنها بارگذاری زلزله افزایش می‌یابد. بیشترین جابجایی در خاک سیستم نگهداری تونل و نیروها در لاینرهای RC برای بارگذاری ترکیبی زلزله و حرکت قطار نسبت به بارگذاری‌های منفرد است.

کلمات کلیدی: بارگذاری دینامیک، تونل زیرزمینی، مترو قطار، تاریخچه زمانی، زلزله.